Journal of Materials Chemistry
www.rsc.org/materials

Magnetite nanocrystals from a single source metallorganic precursor: metallorganic chemistry *vs.* biogeneric bacteria†

Serena A. Corr,[a] Yurii K. Gun'ko,*[a] Alexios P. Douvalis,[b] Munuswamy Venkatesan[b] and Robert D. Gunning[b]

[a]*The Department of Chemistry, Trinity College, University of Dublin, Dublin 2, Ireland*
[b]*The Department of Physics, Trinity College, University of Dublin, Dublin 2, Ireland*

Received 5th January 2004, Accepted 9th February 2004
First published as an Advance Article on the web 23rd February 2004

Magnetite nanocrystals, which are normally formed by magnetogeneric bacteria, have been prepared using a single source metallorganic precursor.

Research on magnetic nanoparticles of magnetite (Fe_3O_4) and maghemite (γ-Fe_2O_3) is of great importance and interest because of their applications in magnetic recording devices[1,2] and biomedical research.[3–5] Ordered systems of magnetite nanocrystals are also found widely in nature, including biological organisms.[6] For example single-domain biogenic magnetite nanocrystals with a size distribution of 35–120 nm may be formed intracellularly *via* a biologically controlled mineralisation process in terrestrial magnetotactic bacteria, such as the MV-1 strain.[7] The magnetosomes (grains of magnetic minerals) arrange themselves in a chain-like structure, which are then attached within the bacterium *via* an unknown anchor-like element. These chains within the bacterium act as a magnetic system for orientation. Magnetostatic interactions between these crystals in the chains result in the formation of a permanent magnetic dipole. These nanocrystals may take a variety of morphologies, of which the hexa-octahedral type are arguably most interesting. This biomineralisation process has also been found to occur in the human brain, which might provide a theory for the mechanism of interaction of environmental magnetic fields with the human central nervous system.[8] Nanocrystalline magnetite has also been discovered in iron-rich extracts from disrupted grass cells.[9]

The past few years has seen growing interest in the size, structure, and arrangement of nanosized magnetite crystals from the Martian meteorite ALH84001.[10,11] These Martian magnetites have similar physical and chemical properties to terrestrial magnetotactic bacteria, including the MV-1 strain.[12] There has been much debate as to whether these truncated hexa-octahedral magnetite nanocrystals provide evidence of former life on Mars. The argument lies in the exact determination of their morphology and shape. As reported by Thomas-Keprta *et al.*, "there are no known reports of inorganic processes to explain the observation of truncated hexa-octahedral magnetites in a terrestrial sample".[10] Recently, Golden *et al.*[13] reported the preparation of magnetite nanocrystals with a morphology corresponding to that of the MV-1 strain. This method involves the thermal decomposition of iron-rich carbonates by heating up to 470 °C and yields nanocrystals with a mean particle length of 52 ± 19 nm. Here, we present a quick and easy one-step sol–gel low temperature synthesis of magnetite nanocrystals using a single source metallorganic precursor. The size distribution and shape of the magnetite nanocrystals are identical to those produced normally by magnetogeneric bacteria and to those found in the Martian sample.[10]

Traditionally, spherical magnetite nanoparticles have been synthesised by a co-precipitation of Fe(II) and Fe(III) salts in ammonium hydroxide solution.[14] Magnetite nanocrystals have also been formed by heat treatment of glass containing iron oxide.[15] Recently, new sol–gel methods have been developed for preparation of magnetite nanocrystals using metallorganic precursors.[16,17] Previously we reported the preparation of the first iron(II) heterometallic alkoxide $[(THF)NaFe(O^tBu)_3]_2$,[18] which is now employed in the preparation of magnetite nanocrystals. The main advantage of this method is that it is a quick, one step low temperature hydrolysis (under ultrasound) of the Fe(II) *tert*-butoxide precursor without using any additional reagents. $[(THF)NaFe(O^tBu)_3]_2$ can be easily prepared by reaction of one equivalent of $FeBr_2$ with three equivalents of sodium *tert*-butoxide in THF.[18] In this work, the solution of the $[(THF)NaFe(O^tBu)_3]_2$ precursor in THF was first hydrolysed with doubly distilled water (Scheme 1). The subsequent ultrasonic and thermal (40–50 °C) treatment for two hours afforded a black precipitate. The residual aqueous solution was found to have a basic pH of 10. The precipitate was washed several times with doubly distilled water, then with ethanol and finally dried under vacuum at room temperature.‡ The product was characterised by X-ray powder diffraction (XRD), transmission (TEM) and scanning electron microscopy (SEM), IR and Mössbauer spectroscopy and finally room temperature magnetization measurements.

Reflections of the XRD patterns (2θ from 5 to 70°) for the sample have shown *d* spacing values and relative intensities of the peaks coincident exactly with JCPDS data of magnetite

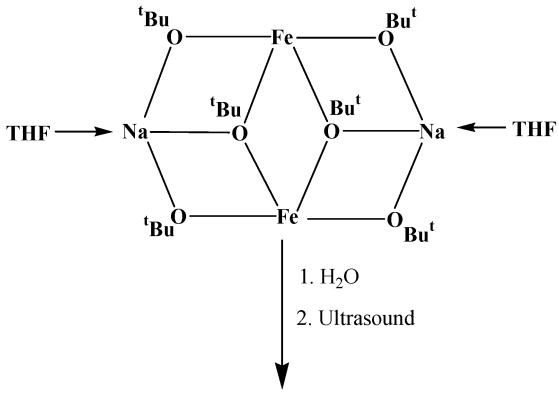

Scheme 1 Preparation of magnetite nanocrystals. *Reagents and conditions*: (i) double distilled water, 1 h; (ii) ultrasound, 40–50 °C, 2 h.

† Electronic supplementary information (ESI) available: Mössbauer spectra of nanocrystals at room temperature (RT), 150 K and 19 K. See http://www.rsc.org/suppdata/jm/b3/b316906e/

DOI: 10.1039/b316906e

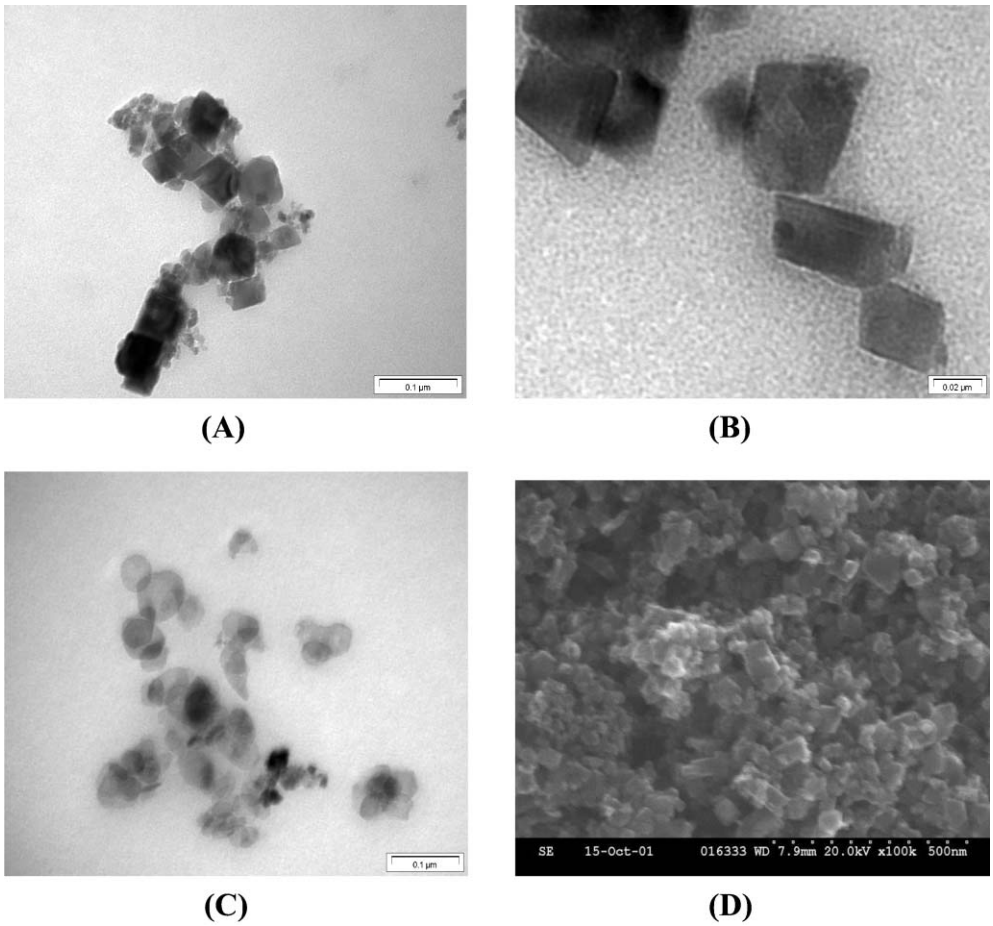

Fig. 1 (A)–(C) TEM images of magnetite nanocrystals taken on a Hitachi H-7000 (100 kV); (D) SEM image of magnetite nanocrystals taken on an S-4300 PC FE SEM.

(Fe_3O_4) with some line broadening. This line broadening is caused by the presence of small particles as shown by the Scherrer formula, which gives a calculated average particle size of 18.3 nm. TEM images of the magnetite sample (Fig. 1 A–C) have shown truncated hexa-octahedral morphology of the magnetite nanocrystals. The average size of the crystals is 25 nm ($N = 100$). A high resolution TEM image of a defect free magnetite nanocrystal has shown magnetite (111) lattice fringes of 4.8 Å. Scanning electron microscopy (SEM) images (Fig. 1 D) confirm the uniform nanocrystalline morphology of the entire sample. IR spectroscopy has shown characteristic peaks of magnetite at 560 cm^{-1} as well the presence of an OH stretch at 3430 cm^{-1}. This indicates that there are some hydroxyl groups on the surface of the magnetite nanocrystals.

The Mössbauer spectra of the nanocrystals were recorded at room temperature (RT), 150 K and 19 K.† A set of five components was used to fit the RT spectrum, and the fitted Mössbauer parameters (MP) suggest the presence of magnetite nanoparticles in a distribution of different sizes. Isomer shift (IS—relative to α-Fe at RT) and hyperfine magnetic field (B_{hf}) values of the pair of two well defined magnetically split sextets with relatively narrow lines and almost zero quadrupole shifts (2ε) are 0.30 mm s^{-1}, 48.3 T and 0.64 mm s^{-1}, 45.3 T respectively. These components correspond to the Fe^{3+} (A) and $Fe^{2.5+}$ (B) sites of relatively large (>130 nm) bulk magnetite crystals. The absorption area ratio of these components is around 1 : 1 suggesting a non-stoichiometric $Fe_{3-x}O_4$ phase. There is a broad magnetically split sextet with IS of 0.40 mm s^{-1} and B_{hf} of 41.5 T. The intermediate IS (between 0.30 mm s^{-1} and 0.64 mm s^{-1}) and the low B_{hf} values can be attributed to magnetite particles with sizes quite close, but above the superparamagnetic limit (6–10 nm)[19,20] at RT. Merging of the A and B site components is a striking characteristic for magnetite nanoparticles of this size.[20] However, this broad component may probably contain contributions from the distorted B site iron ions on the grain boundaries of the larger size particles. In addition, there are two more components—a narrow superparamagnetic component and a magnetically collapsing broad component with IS values of 0.29 mm s^{-1} and 0.38 mm s^{-1} respectively. These correspond to $Fe_{3-x}O_4$ nanoparticles with sizes between 6 and 10 nm and below the superparamagnetic size limit (<6 nm). The lower IS value of the component corresponding to the superparamagnetic particles suggests a composition close to maghemite (γ-Fe_2O_3). The absorption areas are 31%, 21%, 29% and 19% for the bulk particles, the intermediate sized ones, the particles with sizes in the range of the superparamagnetic size limit and the superparamagnetic particles respectively. The characteristics of the Mössbauer spectra for each group of nanoparticles are in good agreement with earlier reports on magnetite nanoparticles of different size distribution.[20]

At 150 K, the lines start to broaden and the central paramagnetic contribution disappears. This suggests a change in the superparamagnetic relaxation, as seen in the characteristic Mössbauer measurement-time-window ($\sim 10^{-8}$ s), which causes the appearance of non-zero hyperfine magnetic splitting for the smaller particles. A set of four components with broad lines was used to fit the spectrum. The first three components correspond to those referred to in the RT spectra. The IS and B_{hf} values are increased compared to the values at RT, as expected. The fourth component contains the merged contributions of the smaller particles. All absorption areas (30% bulk, 19% intermediate, 51% small nanoparticles) are in agreement with the corresponding RT values. At 19 K, the spectrum remains broad, with no indication of a superparamagnetic component. Three components were used to fit the spectra.

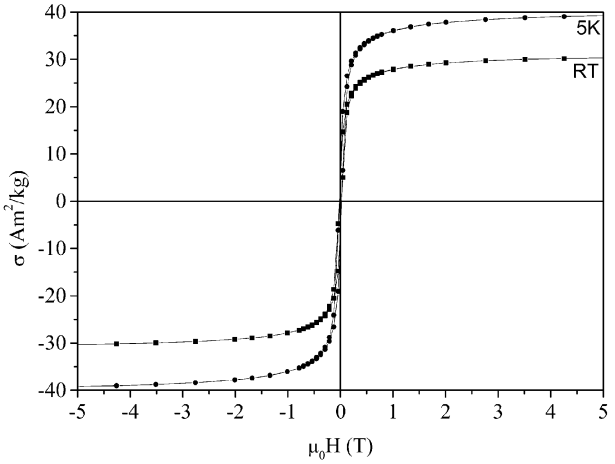

Fig. 2 Magnetisation curves of the magnetite nanocrystals collected at room temperature and 5 K.

Two of them correspond to Fe^{3+} and Fe^{2+} ions of the large $Fe_{3-x}O_4$ particles of the charge ordered phase. The third component with average IS and lower B_{hf} values represents the smaller particles where charge ordering is not achieved at this temperature. The absorption areas are 60% and 40% respectively, in good agreement with the results obtained for the RT and 150 K spectra.

The magnetization curves of the nanoparticles measured at RT and 5 K in a magnetic field of up to 5 T are compared in Fig. 2. The magnetization at 5 K is 1.6 μ_B f.u.$^{-1}$ (39 A m^2 kg^{-1}), much less than the value of 4.0 μ_B f.u.$^{-1}$ anticipated for a bulk half-metallic ferrimagnetic configuration of Fe^{3+} and Fe^{2+} ions. The magnetization is unsaturated even at 5 T. The reduction and lack of saturation could be attributed to the particle size effect, surface spin disorder and probably the presence of antiphase boundaries.[21] The antiferromagnetically coupled spins at the boundary align perpendicular to the applied field and do not contribute to the magnetization.

We suggest that the mechanism of growth of the magnetite nanocrystals involves first hydrolysis of the [(THF)NaFe(O^{t}Bu)$_3$]$_2$ precursor which results in the formation of iron(II) and sodium hydroxides and *tert*-butanol. The process of the magnetite crystallisation was found to be strongly dependent on the pH. The basic pH (10) was necessary for the formation of magnetite nanocrystals in this case. Previously[17] we have shown that hydrolysis of iron(II) alkoxide precursor at neutral (5–6) pH gave only spherical amorphous magnetite nanoparticles. In this work, the heterometallic iron alkoxide [(THF)NaFe(O^{t}Bu)$_3$]$_2$ was a very convenient single source precursor, providing not only iron oxide but also sodium hydroxide for the pH control. The ultrasonic treatment is also important in this preparation. Pure ultrasound produces its effect through cavitation bubbles, which are thought to be the cause of erosion of particles in the vicinity of these bubbles. As water is the solvent in the experiment, the maximum bubble core temperature that can be reached is 4000 K, which causes the pyrolysis of water to H and OH radicals. These radicals have been reported to form hydrogen peroxide, which may contribute to the oxidation of iron(II) oxides to Fe(III).[16]

Thus in this work the use of a metallorganic single source precursor and low temperature sol–gel processing allowed us to prepare magnetite nanocrystals of a morphology analogous to that adopted by both terrestrial and Martian magnetotactic bacteria. Mössbauer spectroscopy and TEM results are consistent with a broad size distribution of nanocrystals, similar to those produced by biologically controlled mineralisation processes in terrestrial magnetotactic bacteria.

Acknowledgements

We gratefully acknowledge staff members of the Electron Microscopy Unit of Trinity College Dublin for their kind support during this work. This work is supported by the Enterprise Ireland Research Innovation Fund (IF-2001-364).

Notes and references

‡ **Preparation of magnetite nanocrystals**: [(THF)NaFe(O^{t}Bu)$_3$]$_2$ was prepared according to the previously published procedure.[18] A solution of [(THF)NaFe(O^{t}Bu)$_3$]$_2$ (6.07 g; 8.2 mmol) in THF (100 ml) was carefully hydrolysed with doubly distilled water (60 ml). The resultant mixture was stirred for one hour, then the reaction vessel was placed in an ultrasonic bath (30 kHz, 130 W) at 40–50 °C for two hours. The black precipitate was filtered and washed three times with distilled water and it was dried in vacuum for 1 day at room temperature (yield: 1.13 g, 89%).

1 R. F. Service, *Science*, 2000, **287**, 1902.
2 F. E. Kruis, H. Fissan and A. Peled, *J. Aerosol Sci.*, 1998, **29**, 511.
3 J. Roger, J. N. Pons, R. Massart, A. Halbreich and J. C. Bacri, *Eur. Phys. J. Appl. Phys.*, 1999, **5**, 321.
4 C. Bergemann, D. Muller-Schulte, J. Oster, L. Brassard and A. S. Lubbe, *J. Magn. Magn. Mater.*, 1999, **194**, 45.
5 A. Jordan, R. Scholz, P. Wust, H. Fahling and R. Felix, *J. Magn. Magn. Mater.*, 1999, **201**, 413.
6 M. Hanzlik, C. Heunemann, E. Holtkamp-Rötzler, M. Winklhofer, N. Peterson and G. Fliessner, *Biometals*, 2000, **13**, 325.
7 B. Devouard, M. Pósfai, X. Hua, D. A. Bazylinski, R. B. Frankel and P. R. Buseck, *Am. Mineral.*, 1998, **83**, 1387.
8 J. L. Kirschvink, M. M. Walker and C. E. Diebel, *Curr. Opin. Neurobiol.*, 2001, **11**, 462.
9 M. Gajdardziska-Josifovska, R. G. McClean, M. A. Schofield, C. V. Sommer and W. F. Kean, *Eur. J. Mineral.*, 2001, **13**, 863.
10 K. L. Thomas-Keptra, S. J. Clemmet, D. A. Bazylinski, J. L. Kirschvink, D. S. McKay, S. J. Wentworth, H. Vali, E. K. Gibson, M. F. McKay and C. S. Romanek, *Proc. Natl. Acad. Sci. USA*, 2001, **98**, 2164.
11 P. R. Buseck, R. E. Dunin-Borkowski, B. Devouard, R. B. Frankel, M. R. McCartney, P. A. Midgley, M. Pósfai and M. Weyland, *Proc. Natl. Acad. Sci. USA*, 2001, **98**, 13490.
12 S. J. Clemett, K. L. Thomas-Keprta, J. Shimmin, M. Morphew, J. R. McIntosh, D. A. Bazylinski, J. L. Kirschvink, S. J. Wentworth, D. S. McKay, H. Vali, E. K. Gibson and C. S. Romanek, *Am. Mineral.*, 2002, **87**, 1727.
13 D. C. Golden, D. W. Ming, C. S. Schwandt, H. V. Lauer, R. A. Socki, R. V. Morris, G. E. Lofgren and G. A. McKay, *Am. Mineral.*, 2001, **86**, 370.
14 X.-P. Qui, *Chin. J. Chem.*, 2000, **18**, 836.
15 U. Lembke, A. Hoell, R. Kranold, R. Müller, W. Schnüppel, G. Goerigk, R. Gilles and A. Wiedenmann, *J. Appl. Phys.*, 1999, **85**, 4.
16 R. Vijaya Kumar, Yu. Koltypin, Y. S. Cohen, D. Aurbach, O. Palchik, I. Felner and A. Gedanken, *J. Mater. Chem.*, 2000, **10**, 1125.
17 G. B. Biddlecombe, Y. K. Gun'ko, J. M. Kelly, S. C. Pillai, J. M. D. Coey, M. Venkatesan and A. P. Douvalis, *J. Mater. Chem.*, 2001, **11**, 2937.
18 Y. K. Gun'ko, U. Cristmann and V. G. Kessler, *Eur. J. Inorg. Chem*, 2002, **5**, 1029.
19 S. Morup, H. Topsoe and J. Lipka, *J. Phys.*, 1976, **37**, C6–287.
20 G. F. Goya, T. S. Berquo, F. C. Fonseca and M. P. Morales, *J. Appl. Phys.*, 2003, **94**, 3520.
21 D. T. Margulies, F. T. Parker, M. L. Rudee, F. E. Spada, J. N. Chapman, P. R. Aitchison and A. E. Berkowitz, *Phys. Rev. Lett.*, 1997, **79**, 5162.